Molecular mechanism of voltage sensing in voltage-gated proton channels

Carlos Gonzalez,[1,2] Santiago Rebolledo,[1] Marta E. Perez,[1] and H. Peter Larsson[1]

[1]Department of Physiology and Biophysics, University of Miami, Miami, FL 33136
[2]Centro Interdisciplinario de Neurociencia de Valparaíso, Universidad de Valparaíso, Valparaíso 2360103, Chile

Voltage-gated proton (Hv) channels play an essential role in phagocytic cells by generating a hyperpolarizing proton current that electrically compensates for the depolarizing current generated by the NADPH oxidase during the respiratory burst, thereby ensuring a sustained production of reactive oxygen species by the NADPH oxidase in phagocytes to neutralize engulfed bacteria. Despite the importance of the voltage-dependent Hv current, it is at present unclear which residues in Hv channels are responsible for the voltage activation. Here we show that individual neutralizations of three charged residues in the fourth transmembrane domain, S4, all reduce the voltage dependence of activation. In addition, we show that the middle S4 charged residue moves from a position accessible from the cytosolic solution to a position accessible from the extracellular solution, suggesting that this residue moves across most of the membrane electric field during voltage activation of Hv channels. Our results show for the first time that the charge movement of these three S4 charges accounts for almost all of the measured gating charge in Hv channels.

The Journal of General Physiology

INTRODUCTION

Voltage-gated proton (Hv) channels are found in phagocytes, neurons, airway epithelia, muscle, and sperm (Decoursey, 2003; Okochi et al., 2009; Ramsey et al., 2009; Iovannisci et al., 2010; Lishko et al., 2010). In phagocytes, Hv channels play an essential role in bacterial clearing. Depolarization-activated H^+ currents through Hv channels in the phagosomal membrane compensate for NADPH oxidase currents, activated during a process called respiratory burst, ensuring sustained production of reactive oxygen species in phagocytes to neutralize engulfed bacteria. The importance of Hv channels is supported by the observation that inhibiting Hv channels prevents further production of reactive oxygen species in the phagosomes. In addition, Hv1 knockout mice are unable to efficiently clear bacterial infections, further showing the essential role Hv channels play in bacterial clearing (Ramsey et al., 2009). Because the voltage dependence of Hv channels determines their physiological role, it is important to determine the molecular structure that defines the voltage sensitivity of Hv channels. At present, it is unknown which charged residues underlie the voltage dependence of Hv channels. Here, using the limiting slope method and accessibility experiments, we have identified the charged residues responsible for voltage activation of Hv channels.

Each subunit in an Hv channel has four transmembrane segments, called S1–S4 (Ramsey et al., 2006; Sasaki et al., 2006). These four transmembrane segments of the Hv channels are homologous to the first four transmembrane segments in voltage-gated potassium (Kv) channels (Ramsey et al., 2006; Sasaki et al., 2006). In Kv channels, the first four transmembrane segments form the voltage-sensing domain, whereas the fifth and the sixth transmembrane segments from all four Kv subunits together form the potassium-conducting pore domain (Jiang et al., 2003; Long et al., 2005). In contrast, Hv channels do not have a fifth or sixth transmembrane segment. In addition, unlike the tetrameric structure of Kv channels, Hv channels are composed of two subunits (Koch et al., 2008; Lee et al., 2008; Tombola et al., 2008). Deletion of the cytosolic domains removes the dimerization of the Hv subunits (Koch et al., 2008; Tombola et al., 2008). Interestingly, the monomeric Hv channel is a functional voltage-gated proton channel. Thus, each subunit comprises a voltage-gated H^+ permeation pathway (Koch et al., 2008; Tombola et al., 2008).

In Kv channels, the fourth transmembrane segment (S4) contains many positively charged residues and has been shown to function as the main voltage sensor in Kv channels (Aggarwal and MacKinnon, 1996; Larsson et al., 1996; Mannuzzu et al., 1996; Seoh et al., 1996; Yang et al., 1996; Tombola et al., 2006). S4 in Hv channels

C. Gonzalez and S. Rebolledo contributed equally to this paper.
Correspondence to H. Peter Larsson: Plarsson@med.miami.edu; or Carlos Gonzalez: carlos.gonzalezl@uv.cl

Abbreviations used in this paper: FEP, free energy perturbation; MD, molecular dynamics; MTSEA, 2-aminoethyl MTS; MTSET, 2-(trimethylammonium)ethyl MTS; MTSPT, 3-(trimethylammonium)propyl MTS.

The Rockefeller University Press $30.00
J. Gen. Physiol. Vol. 141 No. 3 275–285
www.jgp.org/cgi/doi/10.1085/jgp.201210857

contains just three charged arginine residues compared with, for example, seven charged residues in Shaker K^+ channels (Fig. 1 A). A cysteine accessibility study of cysteines introduced in S4 of Hv channels shows that S4 undergoes a voltage-dependent transmembrane movement during gating, suggesting that the positive charges on S4 are part of the voltage sensor that controls Hv channel gating (Gonzalez et al., 2010). However, that study only shows that S4 movement is correlated with channel opening and not that the S4 charges are the underlying gating charges. To demonstrate the role of the S4 positively charged residues with some direct methodology is important given that other studies showed that individual neutralizations of the second and third S4 charges did not significantly decrease the voltage dependence of Hv channels, when measured as changes in the slope of conductance versus voltage curves at the midpoint of activation (Ramsey et al., 2006; Sasaki et al., 2006). Neutralizations of the first S4 charge increased the voltage dependence of Hv channels in one study (Sasaki et al., 2006) but decreased the voltage dependence in the other study (Ramsey et al., 2006). In addition, Hv channels truncated between the second and third charge in S4 still generated voltage-gated proton currents (Sakata et al., 2010). Therefore, the question of how much the three S4 arginines contribute to voltage sensing and effective gating charge in Hv channels is open at present. Here we test the effect of neutralizing each of the three arginines in S4 to determine their contribution to the effective gating charge in Hv channels by the more accurate method of measuring the gating charge in the limit of very small channel open probability (i.e., the limiting slope method; Almers, 1978; Sigg and Bezanilla, 1997).

MATERIALS AND METHODS

Mutagenesis and expression

Site-directed mutagenesis, cRNA transcription, and injection of cRNA encoding *Ciona intestinalis* Ci-VSOP (here called Ci-H_V) into *Xenopus laevis* oocytes were performed as described previously (Sasaki et al., 2006; Bruening-Wright et al., 2007). The ΔNΔC Ci-H_V has a stop codon at Val270 and initiator methionine replacing Glu129 (Gonzalez et al., 2010).

Cysteine accessibility

Cysteine accessibility to MTS reagents in excised inside-out patch clamp and two-electrode voltage clamp (TEVC) experiments was assessed as described earlier (Gonzalez et al., 2010) using MTSEA (2-aminoethyl MTS), MTSET (2-(trimethylammonium)ethyl MTS), or MTSPT (3-(trimethylammonium)propyl MTS). TEVC external solution contained (in mM) 88 NaCl, 1 KCl, 1 $MgCl_2$, 1 $CaCl_2$, and 100 HEPES, pH 7.4. Currents were recorded using a Dagan CA-1B amplifier (Dagan Corporation), low-pass filtered at 1 kHz, and sampled at 5 kHz. Oocytes were injected with 50 nl of 1M HEPES, pH 7.0, to minimize pH changes caused by the proton currents. This results in a concentration of ∼100 mM HEPES in the cytosol. 1M-HEPES injection prevents the internal pH from changing significantly by the proton currents (Gonzalez et al., 2010). Both pipette and bath solutions for excised patch recordings contained (in mM) 100 HEPES, 2 $MgCl_2$, and 1 EGTA, pH 7 with NMDG. Currents were recorded using an Axopatch 200B amplifier (Molecular Devices), low-pass filtered at 1 kHz, and sampled at 5 kHz. To increase the proton currents in some recordings, we used pH_i 5.5 (and Mes instead of HEPES). The rate of MTS modification was only determined using patches where solution exchange was <100 ms (e.g., Fig. 4 D; Larsson et al., 1996). The rate of modification was measured by plotting the change in the current by the MTS reagent as a function of the exposure to the MTS reagents (exposure = concentration × time, measured in [mM s]; e.g., Fig. 4 G). The current versus exposure plot was then fit with an exponential to get the second order rate constant (unit/mM/s) of the MTS reaction.

Limiting slope theory

For a two-state voltage-gated channel (one closed state and one open state), the gating charge z can be estimated by fitting the conductance versus voltage, G(V), curve by a Boltzmann: $G(V) = G_0/(1 + \exp(-z(V - V_{1/2})/kT))$. Alternatively, one can plot the G(V) curve in a log-lin plot and fit the slope at small open probabilities, i.e., the limiting slope technique (Almers, 1978; Sigg and Bezanilla, 1997). This is because at low open probabilities, $\log G(V) \rightarrow \log G_0 + zV/kT$. For channels with more states than two, the fit of the G(V) with a Boltzmann only gives a lower estimate of the total gating charge, z_{total}, needed to move to activate the channel. For example, a Hodgkin-Huxley type channel with only two subunits and a gating charge $z = 2\ e_0$ per subunit (Fig. 1 B, inset) has a $G(V) = G_0/(1 + \exp(z(V - V_{1/2})/kT))^2$. The G(V) from this two-subunit channel is not well fit with a Boltzmann (Fig. 1 B, red dashed line), and the fit gives a lower z value ($z_{fit} = 2.43\ e_0$) than the real total gating charge per channel z_{total} ($z_{total} = 2\ e_0 + 2\ e_0 = 4\ e_0$). Fitting the G(V) with a Boltzmann raised to a power of two ($z_{fit} = 2\ e_0$) or three ($z_{fit} = 1.87\ e_0$) fits the G(V) much better (Fig. 1 B, solid red and dashed teal line, respectively). Fitting the G(V) with a Boltzmann raised to a power of two or three is equivalent to assuming that the channel has two or three identical subunits (in a Hodgkin-Huxley type channel), respectively. In this case, the fitted z_{fit} is per subunit and the total estimated charge per channel z_{total} is two times z_{fit} for the Boltzmann to the second power ($z_{total} = 2 \times 2\ e_0 = 4\ e_0$) and three times z_{fit} for the Boltzmann to the third power ($z_{total} = 3 \times 1.87\ e_0 = 5.6\ e_0$). From this it is clear that the fits of the G(V) with a simple Boltzmann underestimate the true total gating charge, whereas fitting with higher powers of a Boltzmann could lead to overestimates of the true gating charge. In contrast, the limiting slope technique is less model dependent and will for most models give a good estimate of the equivalent gating charge, if the slope is measured at low enough open probabilities. For example, for the two-subunit model, the $\log G(V) \rightarrow \log G_0 + 2zV/kT$ for low open probabilities. Using the limiting slope technique for simulated data down to a open probability of 10^{-3}, the fit to the three-state channel gives a $z_{limit} = 3.8\ e_0$ (Fig. 1 C, teal line), close to the correct value, $z_{total} = 4\ e_0$.

Limiting slope experiments

To measure the limiting slope, currents were recorded from excised inside-out patches containing WT or charge-neutralized Ci-Hv1 channels in response to slow ramps of voltage (1–2 mV/s) from a holding potential of −60 to 40 mV (or 0 mV) and back to −60 mV (e.g., Fig. 1 D). Solutions for excised patch recordings contained (in mM) 100 HEPES, 2 $MgCl_2$, and 1 EGTA, pH 7 with NMDG, in pipette and 100 Mes, 2 $MgCl_2$, and 1 mM EGTA, pH 5.5 with NMDG, in bath solution. Currents were recorded using an Axopatch 200B amplifier, low-pass filtered at 1 kHz, and sampled at 2 kHz. Up to 20 current traces were averaged and low-pass filtered at 5 Hz to improve the signal to noise. There were no significant endogenous currents in response to the voltage ramps (Fig. 1 D, teal line), most likely because of the almost complete

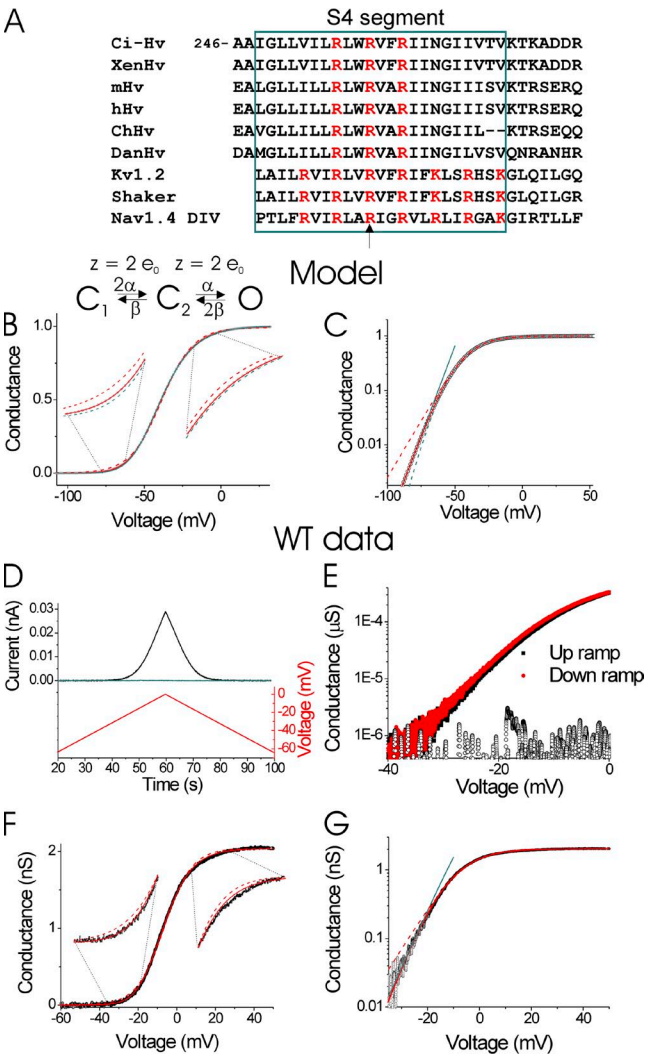

Figure 1. Limiting slope estimates the effective gating charge. (A) Alignment of the S4 region (teal box) of Hv channels from *C. intestinalis* (Ci-Hv), *Xenopus* (XenHv), *Mus musculus* mouse (mHv), *Homo sapiens* (hHv), *Gallus gallus* (ChHv), and *Danio rerio* (DanHv) and S4 from Kv1.2, *Shaker* K, and domain IV of Nav1.4 channels. The arrow shows residues R1454 in Nav1.4 and R368 in Shaker that have been shown to move completely across the membrane during channel activation (Yang et al., 1996; Baker et al., 1998). Red letters indicate positively charged residues in S4. (B) Simulated conductance versus voltage, G(V), curve (black circles) for a three-state, two-subunit Hodgkin-Huxley type model with a gating charge of z = 2 e_0 per subunit. The G(V) was fit with a Boltzmann curve, $G(V) = G0/(1 + \exp(-z(V - V_{1/2})/kT))$ (z_{fit} = 2.43 e_0; dashed red line), and a Boltzmann curve to the second (z_{fit} = 2.0 e_0, resulting in a $z_{total}(fit) = 2 \times z_{fit}$ = 4.0 e_0; red line) and third power (z_{fit} = 1.87 e_0, resulting in a $z_{total}(fit) = 3 \times z_{fit}$ = 5.6 e_0; teal dashed line). (C) Simulated data and fits from B shown in lin-log plot (colored as in B). Also the best fit to the limiting slope at negative voltages is shown (log G(V) = constant + $z_{limit}V/kT$; $z_{limit}(fit)$ = 3.8 e_0; teal straight line). (D) Currents from excised patches containing WT Ci-Hv1 channels (black line) or from patches taken from uninjected oocytes (teal line) in response to slow voltage ramps (1.5 mV/s) from −60 to 0 mV and then back to −60 mV. (E) The calculated conductance ($I/(V - E_{rev})$) during the up and down ramp (data from D). Also shown is the calculated conductance from a patch from an uninjected oocyte (open circles). The currents were leak subtracted in response to ramps between −100 and −80 mV. The reversal potential E_{rev} was estimated to −85 mV in this experiment (pH_i = 5.5 and pH_o = 7). Note that the conductance estimated during the up ramp overlaps with the conductance during the down ramp, showing that the channels are at equilibrium at all voltages. This shows that the speed of the ramp is slow enough to correctly estimate the conductance. (F and G) Conductance, G, measured as in D from excised patches containing WT Ci-Hv1 channels in response to slow voltage ramps (1.5 mV/s) from −60 to 50 mV. The G(V) was fit with a Boltzmann curve, $G(V) = G0/(1 + \exp(-z(V - V_{1/2})/kT))$ (z_{fit} = 3.5 e_0; dashed red line), and a Boltzmann curve to the second power, $G(V) = G0/(1 + \exp(-z(V - V_{1/2})/kT))^2$ (z_{fit} = 3.0 e_0, resulting in a $z_{total}(fit) = 2 \times z_{fit}$ = 6.0 e_0; solid red line). (G) Data and fits from F shown in lin-log plot (colored as in F). Also the best fit to the limiting slope at negative voltages is shown (log G(V) = constant + $z_{limit}V/kT$; teal straight line). $z_{limit}(fit)$ = 5.3 e_0.

absence of any ions permeable to endogenous oocyte channels in these patch solutions. Currents were leak subtracted for ramps between −100 and −80 mV. We calculated conductance versus voltage, G(V), curves by dividing the currents by $(V - E_{rev})$. The conductance-voltage curves from up and down ramps were indistinguishable, as expected when the channels are near gating equilibrium during the measurements (Fig. 1 E). G(V)s of WT Hv1 channels were not well fit by a simple Boltzmann (Fig. 1, F and G, dashed red lines). Instead, we plotted the conductance on a semi-logarithmic scale (Fig. 1 G), and the G(V)s were fitted in different voltage intervals to identify the limiting logarithmic slope, as described earlier (Gonzalez et al., 2010).

RESULTS

The effective gating charge is reduced by S4 neutralizations

We studied the Hv1 channel from the sea squirt *C. intestinalis*, Ci-VSOP or Ci-Hv1, because these channels can be expressed at higher densities in *Xenopus* oocytes than their mammalian Hv1 homologues. The higher densities of Ci-Hv1 channels expressed in oocytes enabled us to more reliably measure the proton currents at low open probabilities, as necessary for the limiting slope technique. The effective gating charge of WT Ci-Hv1 channels is 5.9 e_0 (dimer) and 2.7 e_0 (monomer), as measured from the limiting slope conductance (see Materials and methods; Gonzalez et al., 2010). The effective gating charge is the amount of charge that needs to move relative to the transmembrane electric field to turn on the proton conductance. The higher value in the dimeric channels is consistent with cooperative activation of the proton conductance in the two subunits (Gonzalez et al., 2010; Tombola et al., 2010). Here, we replaced, one by one, the three arginines on the S4 segment of Hv channels from *C. intestinalis* with asparagines (Fig. 1 A) to determine the contribution of each of the three arginines present in S4 to the gating charge in Hv channels.

To measure the effective gating charge in the arginine mutants, we applied very slow voltage ramps (1–2 mV/s) to inside-out patches from oocytes expressing

the different S4 charge neutralization mutants and measured the resulting currents (Fig. 2 A). The current-voltage curves from up and down ramps were indistinguishable (Fig. 2 B), as expected when the channels are near gating equilibrium during the measurements. We calculated the conductance from these current measurements and plotted the conductance versus voltage curves in semilogarithmic plots (Fig. 2, C–E). The limiting slope at negative voltages has been shown to be an accurate measure of the effective gating charge necessary to open the channel (Almers, 1978). A substantial decrease of the effective gating charge as measured from the limiting slope conductance was measured when R255, R258, or R261 was neutralized compared with the effective gating charge in WT Ci-Hv channels (Fig. 2 F). Double and triple neutralizations of the three S4 charges did not produce functional channels or their expression was too low to conduct patch clamp experiments.

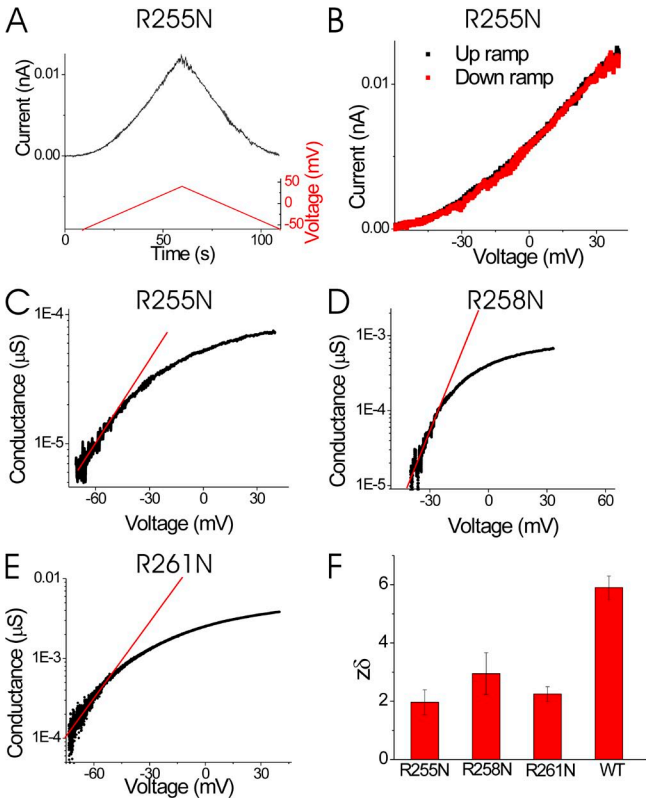

Figure 2. Neutralization of any S4 charge reduces the effective gating charge. (A) Currents from excised patches containing R255N Ci-Hv1 channels in response to slow voltage ramps (2 mV/s) from −60 to 40 mV and then back to −60 mV. (B) The current during the up and down ramp (data from A). (C–E) Conductance (G) calculated as $G = 1/(V - E_{rev})$ from measurements as in A and B from excised patches in response to slow voltage ramps (2 mV/s) for R255N (C), R258N (D), and R261N (E) Hv channels in $pH_i = 5.5$ and $pH_o = 7$. The limiting slope fitted as $G = G_0/e^{z\delta VF/RT}$ is shown for each recording. (F) Effective gating charge (zδ) estimated from the limiting slope for charge-neutralized and WT Hv channels ($n = 4$) from experiments as in A and B. Error bars are SEM.

The reductions in effective gating charge for the single neutralizations suggest that each one of three S4 charges contributes significantly to the voltage sensing of Hv channels. However, a decrease in the effective gating charge caused by the charge neutralizations could also be the result of a change in the dimerization probability or extent of cooperativity of the two Hv subunits. Therefore, we also made the S4 charge neutralization mutations in the form of Hv channels that had the cytosolic domains deleted (ΔNΔC; Koch et al., 2008), a deletion which prevents dimerization (and thereby also abolishes cooperativity). In these monomeric Hv channels, the effective gating charge decreases substantially when R255, R258, or R261 is neutralized (Fig. 3), as if all three S4 charges contribute to the effective gating charge in monomeric as well as dimeric Hv channels.

The S4 movement is curtailed by S4 neutralizations

The reduction in gating charge produced by the neutralizations is surprisingly large (>2 e_0 for dimeric channels and >1 e_0 for monomeric channels), especially for the R255N mutation (Fig. 3 C). A reduction of 1 e_0 per subunit is the maximally expected reduction in the gating charge by the neutralization of one charged residue, assuming that the charge neutralization only removes a charge from S4 and does not alter anything else in the channel. If one adds up the gating charge reduction for all mutations, one gets a total of 12 e_0, a number which is twice the 6 e_0 measured for WT Hv channels. This result suggests that the effect of the neutralizations is not a simple removal of the charged residue. If, in addition, the charge neutralization also reduces the distance moved by the remaining charges in the transmembrane electrical field, then the contribution of the remaining charges to the gating charge will also be reduced. We therefore tested whether some charge reduction in Hv channels also could be caused by an altered S4 movement, especially for the R255N mutation.

We used cysteine accessibility to test for altered S4 movement in the R255N mutation. There are two native cysteines in the N terminus and one native cysteine in the C terminus of *C. intestinalis* Hv1. However, we have previously shown that the currents from WT Ci-Hv1 are not modified by the application of internal or external MTS thiol reagents, such as MTSET or MTSES (2-sulfonatoethyl MTS; Gonzalez et al., 2010). Therefore, we used the WT *C. intestinalis* Hv1 channel as the background for our cysteine mutations and cysteine accessibility experiments. I262C has earlier been shown to be accessible to MTSET from the intracellular solution in closed channels (Fig. 4, A and B; Gonzalez et al., 2010). Modification of I262C by intracellular MTSET abolished the current through I262C channels (Fig. 4 B). We combined I262C with R255N and tested the internal accessibility of I262C in the presence of R255N

(Fig. 4, C–G). Using a fast perfusion system (Fig. 4 D), we were able to apply 1 mM MTSET for 1 s to the intracellular side of the patch. This allowed us to apply MTSET specifically while the channels were held at a specific voltage. We monitored the current from R255N/I262C channels in response to a 100-mV pulse every 10 s, while applying 1 mM MTSET to the cytosolic face of an excised patch for 1 s every 10 s at −100 mV (Fig. 4 E). In contrast to I262C channels (Fig. 4, A and B), internal MTSET did not modify closed R255N/I262C channels (Fig. 4, C–G). Even applying internal MTSET at such a negative voltage as −140 mV did not modify R255N/I262C channels (Fig. 4 G, triangles), as if S4 does not move as far inward toward the cytosol in R255N/I262C channels compared with I262C channels (Fig. 4 H). The decreased range of S4 motion is consistent with the large reduction of the effective gating charge caused by the R255N neutralization (Fig. 2 F). A possible reason for the decreased range of S4 motion is that the two end points of S4 movement are determined by charge–charge interactions of S4 charges with the two clusters of negative residues at the intracellular and extracellular border of the channel (Fig. 4 H; Long et al., 2007). When the most extracellular S4 charge is neutralized (R255N), S4 would only travel as far inward as to make the next S4 charge (R258) interact with the internal negative cluster (Fig. 4 H). I262C would in this S4 position be located at the same place as residue 259 in WT channels, which we previously showed to be inaccessible from the intracellular solution (Gonzalez et al., 2010). A similar mechanism with a reduced outward S4 motion could explain the large reduction in gating charge for the R261N neutralization (Fig. 2 F).

The middle S4 charge moves completely across the membrane

A simple interpretation of the reduction of gating charge for the S4 charge neutralizations (Fig. 2) is that these S4 charges move across most (if not all) of the electrical field during channel activation (Fig. 5, A and B), suggesting that these S4 charges move completely from a cytosolic accessible position to an extracellular accessible position. However, the accessibility experiment above shows that charge neutralizations might alter the extent of the S4 movement, thereby complicating the interpretation of the charge neutralizations. To get further independent evidence that these S4 charges move from the cytosolic side to the extracellular side of the membrane, we also tested the accessibility of R258C, the middle S4 charged residue, to internal membrane-impermeable cysteine reagents (MTSET) in closed and open channels. R258 lies in between two residues, L256 and V259, which we earlier have shown to be inaccessible from both the intracellular and extracellular solutions in both closed and open channels (Gonzalez et al., 2010). However, mapping these residues (L256, R258, and V259) onto existing models for Kv channels in closed and open states suggests that R258 could be accessible from both sides of the membrane, even if 256 and 259 are not accessible from either side of the membrane (Fig. 5, C–F). We therefore decided to test the accessibility of R258C from both sides of the membrane. External accessibility of 258C was tested by applying MTS reagents on whole oocytes expressing R258C Hv1 channels, whereas internal accessibility of 258C was tested by applying MTS reagents on excised inside-out patches from oocytes expressing R258C Hv1 channels.

Internal MTSET modifies R258C channels (Fig. 6, A and B). MTSET slowed the time course of the R258C currents (Fig. 6, A–C). Internal MTSET modified R258C channels when applied at negative potentials ($k = 0.63 \pm 0.04$/mM/s; $n = 7$) but not at positive potentials (Fig. 6, D and E). In contrast, external MTSET did not modify R258C. However, externally applied MTSEA, which is smaller than MTSET, modified R258C channels (Fig. 7, A and B). The membrane-impermeable MTSPT, which has a longer linker between the charge and the thiol

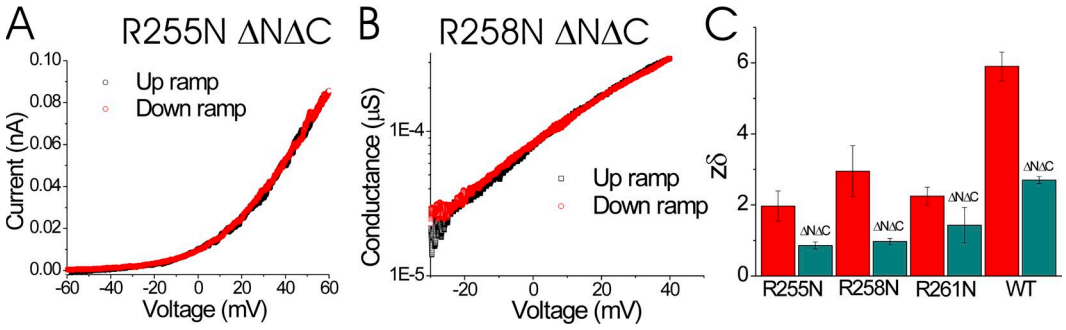

Figure 3. Neutralization of S4 charges reduces the effective gating charge in monomeric Hv channels. (A) The current during up and down voltage ramps for monomeric R255N ΔNΔC Ci-Hv1 channels. (B) The calculated conductance ($I/(V - E_{rev})$) during up and down voltage ramps for monomeric R258N ΔNΔC Ci-Hv1 channels. The conductance is similar during the up and down ramps, showing that the ramp speed is slow enough to estimate the steady-state conductance. (C) Effective gating charge (zδ) estimated from the limiting slope for charge-neutralized and WT Hv channels in dimeric (red) or monomeric (teal) form (ΔNΔC; see Materials and methods; $n = 4$). Error bars are SEM.

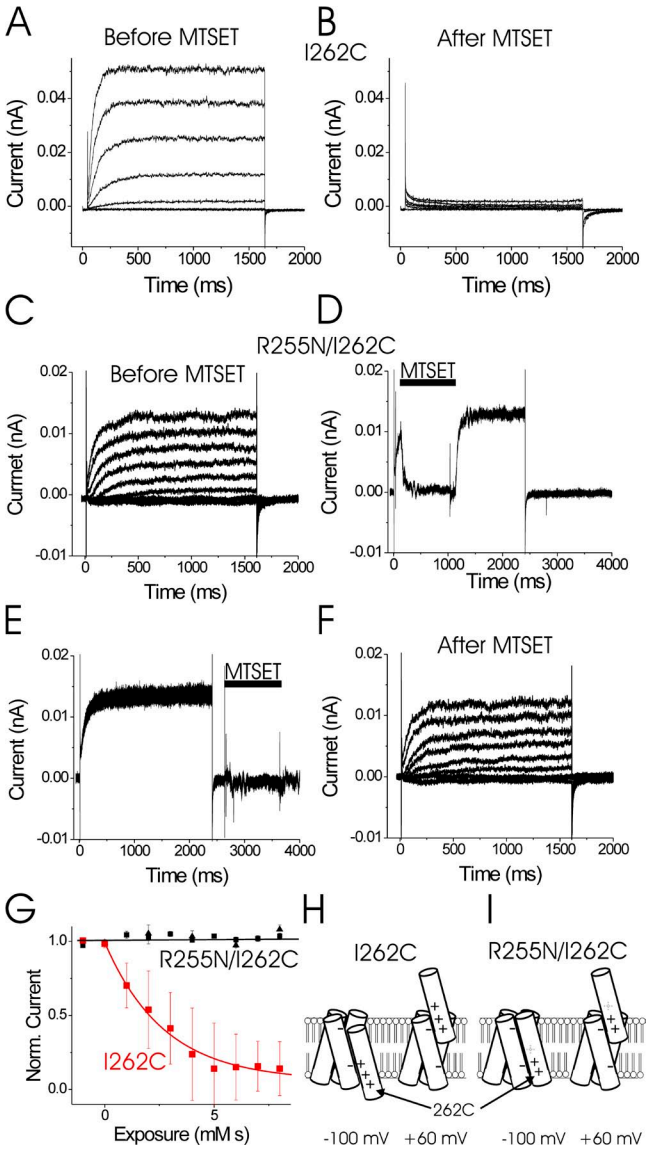

Figure 4. R255N alters the extent of S4 movement. (A and B) Currents from an excised inside-out patch containing I262C channels in response to voltage steps from −40 to 80 mV, before (A) and after (B) application of internal MTSET. 1 mM MTSET was applied for 10 s on closed channels held at −100 mV in between the two recordings. (C and F) Currents from an excised inside-out patch containing R255N/I262C channels in response to voltage steps from −40 to 100 mV (in 20-mV increments), before (C) and after (F) 1 mM MTSET was applied 10 times at −100 mV for 1 s. $pH_i = 5.5$ and $pH_o = 7$. (D) Currents in response to a 100-mV voltage step every 10 s during MTSET application on open R2355N/I262C channels. The speed of the perfusion of the cytosolic face of the patch was tested by applying 1 mM MTSET (in pH 7.0 solution) at 100 mV for 1 s, followed by washout at 100 mV (pH 5.5 solution). Wash-in and washout were monitored by the fast changes in current amplitude induced by changes in internal pH: $pH_i = 5.5$ in rinse and $pH_i = 7.0$ in MTSET solution. $pH_o = 7.0$ (pipette solution). (E) Currents in response to a 100-mV voltage step every 10 s during MTSET application on closed R255N/I262C channels. Closed-state modification was tested by applying 1 mM MTSET at −60 mV for 1 s, followed by washout. Same patch as D. (G) Normalized currents in response to voltage steps to 100 mV after sequential 1-s applications of 1 mM MTSET applied at −100 mV on I262C (red boxes) and R255N/I262C (black boxes) channels, or sequential 1-s applications of 2 mM MTSET applied at −140 mV on R255N/I262C (black triangles) channels. MTSET was only applied during the inter-episode time at a holding voltage of −100 mV (or −140 mV; as in E). Error bars are SEM. (H and I) Cartoon showing proposed interactions of the positively charged S4 residues (R255, R258, and R261) with the two clusters of negatively charged residues in S1–S3 at the intracellular and extracellular borders of the Hv subunit in I262C (H) and R255N/I262C (I) channels. We propose that it is the interactions of the S4 charges with the two negatively charged clusters that set the limits for the extent of S4 movement (Fig. 3 [A and B] from Gonzalez et al., 2010).

reactive end than MTSET, also modified R258C (Fig. 7, C and D). External MTSEA modified 258C channels when applied at depolarized potentials ($k = 0.18 \pm 0.03$/mM/s; $n = 3$) but not at hyperpolarized potentials (Fig. 7 E). The external accessibility data suggest that R258C is located in a narrow extracellular crevice in the open state. The accessibility of R258C from both sides of the membrane, but with opposite voltage dependence, shows that R258C moves from a position accessible from the cytosolic solution in closed channels to a position accessible from the extracellular solution in open channels.

DISCUSSION

We have shown here that neutralizations of individual S4 charges reduce the effective gating charge in Hv channels, as if all three S4 charges contribute to the gating charge. In addition, we show that during Hv channel opening, the displacement of the middle S4 charged residue (R258) encompasses the whole membrane electric field. When channels are closed, this residue is accessible from the cytosolic solution. In contrast, when channels are open, this residue is accessible from the extracellular solution. Assuming that the membrane electrical field falls over the inaccessible portion of the protein, this suggests that R258 contributes 1 e_0 per subunit to the gating charge. In voltage-activated Na channels, it has earlier been shown that a cysteine introduced at the homologous residue to R258 (Fig. 1 A, arrow) can bind MTSET on the extracellular side of the membrane and then the intracellular reducing agent TCEP (Tris (2-carboxyethyl) phosphine) could remove MTSET on the intracellular side, clearly showing that S4 residue modified with MTS reagents can move from one side of the membrane to the other side of the membrane (Yang et al., 1996). Our present data, together with our earlier work in which we showed that the movement of S4 precedes Hv channel opening (Gonzalez et al., 2010), strongly support a model in which the voltage dependence of Hv channels is caused by the movement of the three S4 charges.

Earlier studies of the roles of the three S4 charges in the voltage dependence of Hv channels were inconclusive or contradictory (Ramsey et al., 2006; Sasaki et al., 2006). The conclusions of these studies were based on changes in the Boltzmann fits of the whole conductance versus voltage G(V) curves from different charge-neutralizing mutations (Ramsey et al., 2006; Sasaki et al., 2006). However, the number of gating charges estimated from Boltzmann fits of G(V) curves are only lower estimates of the true gating charge. This is because mutations could change the slope at the midpoint of the G(V) curves by altering the cooperativity between channel subunits and/or altering the relationship of the different activation steps in a multistep activation pathway of the channels, and not just by decreasing the number of gating charges (Zagotta et al., 1994). Therefore, it is very unreliable to use changes in Boltzmann fits to estimate the contribution of individual charges. Instead, here we used the more reliable method of measuring the limiting slope at low conductance to estimate the effective gating charge for the different mutations (Almers, 1978; Sigg and Bezanilla, 1997). However, even the limiting slope technique has limitations. One of the possible errors is to not have measured the conductance at low enough open probability to have reached the true limiting slope. For example, in Nav1.4 channels, the effective gating charge was estimated to 4–7 e_0 per channel from limiting slope experiments on macroscopic currents where the conductance could be estimated down to an open probability of 10^{-3} (Oxford, 1981; Stimers et al., 1985), whereas the effective gating charge was estimated to 12 e_0 per channel from limiting slope experiments on single channel experiments

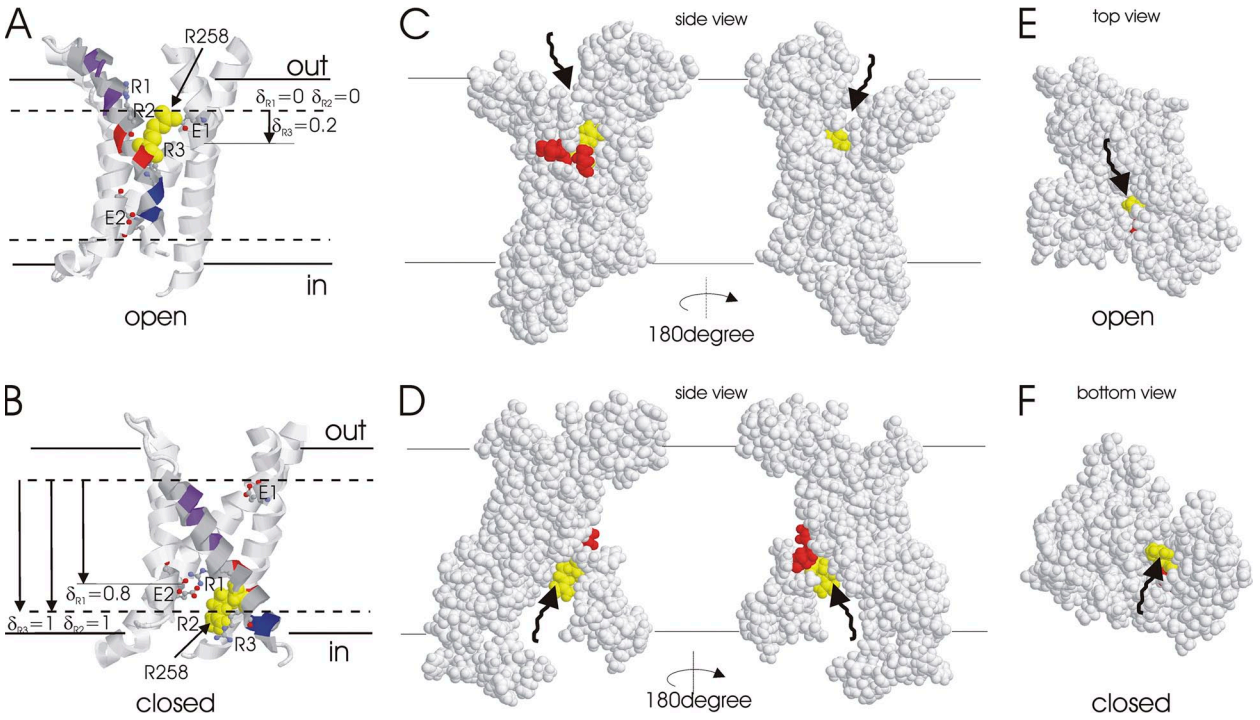

Figure 5. Cysteine accessibility is consistent with an S4 movement in which all three S4 charges significantly contribute to the effective gating charge. (A and B) Proposed S4 movement and charge–charge interactions in WT Hv channels according to present and previous (Gonzalez et al., 2010) cysteine accessibility data mapped onto the voltage-sensing domains from the Kv1.2-2.1 chimera channel structure (Long et al., 2007; A) and a closed-state model of Shaker K channels (Pathak et al., 2007; B). Positively charged S4 residues (R1, R2, and R3) and negatively charged glutamate residues (E1 and E2) are shown as ball and stick (except R2 = R258, which is space filled and colored yellow). Purple residues are only accessible from the extracellular solution in open channels and blue residues from the intracellular solution in closed channels (Gonzalez et al., 2010). Red residues (256 and 259) are not internally or externally accessible in closed or open channels (Gonzalez et al., 2010). Solid lines indicate proposed lipid bilayer boundaries, and dashed lines indicate proposed MTS accessibility as the result of water-filled crevices. Proposed positions of the charges of the three S4 arginine residues relative to the inaccessible portion of S4 are indicated. Assuming that the electrical field falls linearly over the inaccessible portion of S4, R255, R258, and R261 would contribute 0.80 e_0, 1.0 e_0, and 0.80 e_0, respectively, to a total gating charge Q = 2.6 e_0. This is similar to the contributions associated with these charges in FEP/MD simulations on the Kv1.2 voltage-sensing domain (Khalili-Araghi et al., 2010). (C and D) Two side views of the S1–S4 of an Hv1 channel monomer in the open (C) and closed (D) state rotated 180 degrees relative each other are shown in space fill. (E) Top view of the open state shown in C. (F) View from intracellular solution of the closed state shown in D. R258 is shown in yellow, and residues 256 and 259 are shown in red. R258 is accessible from the extracellular surface through a water-filled crevice (C and E) and from the intracellular surface through a water-filled crevice (D and F). Neither residue 256 nor 259 is visible from either side of the membrane in either closed or open states, consistent with earlier accessibility experiments (Gonzalez et al., 2010). Arrows show aqueous access to R258.

where the conductance could be estimated down to an open probability of 10^{-7} (Hirschberg et al., 1995). In principle, there is no way to know that the true limiting slope has been reached in any particular experiment, unless there is another way to estimate the gating charge movement (e.g., from gating currents). Our experiments are limited by the signal to noise at very low open probabilities for macroscopic currents because of the very small single channel conductance of Hv1 channels (Cherny et al., 2003) and because no gating currents have been measured from Hv1 channels. However, the estimated effective gating charge of 6 e_0 in the Ci-Hv1 channel from our limiting slope experiments matches well with the estimated charge transfer caused by the S4 movement measured by our cysteine accessibility experiments (Gonzalez et al., 2010).

The neutralizations of the S4 charges caused surprisingly large reduction in the effective gating charge for the charge neutralization mutants (Fig. 2). A reduction in the measured effective gating charge of only 1 e_0 per subunit is expected for any charge neutralization if the neutralization does not cause any other change to the protein or the applied transmembrane electrical field. One possibility is that we have not reached the true limiting slope for these mutations because of the limiting range of open probabilities in our experiments for these mutations (Figs. 2 and 3). However, in that same open probability range, the slope of the G(V) curve for WT Ci-Hv1 channels has already reached a value that is within 10% of the limiting slope value measured at even lower open probabilities (Fig. 1, E and G; Gonzalez et al., 2010), suggesting that we have not grossly underestimated the gating charge for the mutants. Another possibility is that the assumptions that the neutralization does not cause any other change to the protein or the applied transmembrane electrical field are not necessarily true for all types of mutations. One should be especially concerned about the validity of these assumptions for mutations of charges that are essential for the conformational changes underlying channel gating. If one adds up the gating charge reduction for all mutations, one gets a total of 12 e_0, a number which is twice the 6 e_0 measured for WT Hv channels. However, similar neutralization experiments on Shaker K channels also reduce the total gating charge by >1 e_0 per subunit for some mutations (Aggarwal and MacKinnon, 1996; Seoh et al., 1996). If one adds up the gating charge reduction for all Shaker

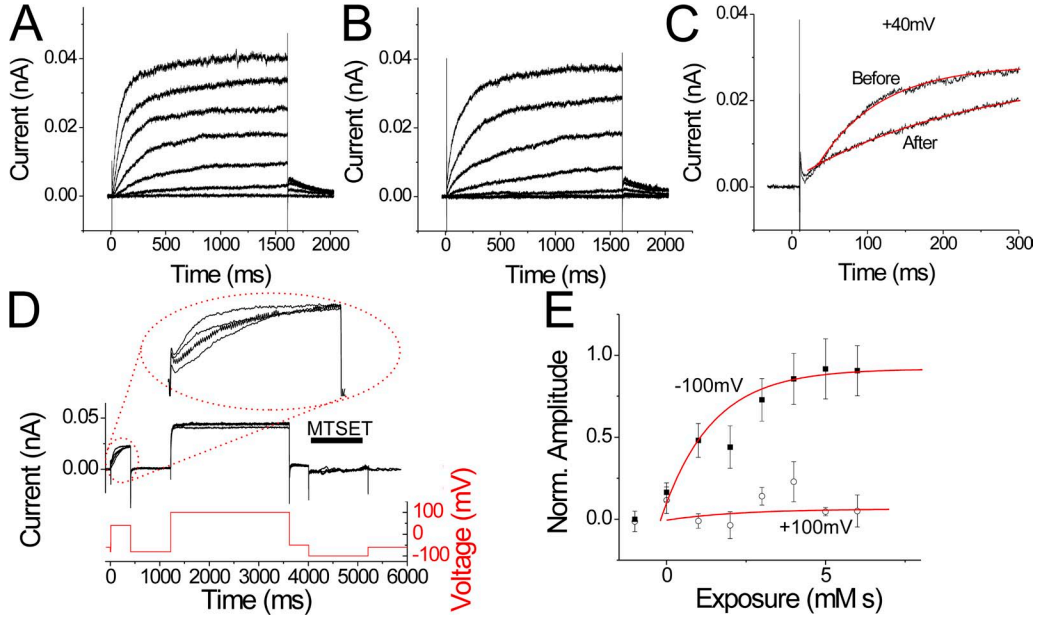

Figure 6. Internal MTSET modifies R258C channels only in the closed state. (A and B) Currents from an excised inside-out patch containing 258C channels in response to voltage steps from −60 to 60 mV, before (A) and after (B) application of internal MTSET (1 mM) for 10 s and washout for 10 s. The holding potential was −60 mV. (C) Currents in response to a voltage step to 40 mV before and after application of internal MTSET. The current time course was fitted with an exponential (red lines) with τ = 70 ms before MTSET and 220 ms after MTSET. (D) Currents from an excised inside-out patch containing R258C channels in response to sequential voltage steps to 40, 100, and −100 mV. $V_{holding}$ = −80 mV. pH_i = 5.5 and pH_o = 7. 1 mM MTSET was applied for 1 s during the −100-mV voltage step. This protocol was repeated every 10 s for 10 times (only four traces are shown for clarity). The inset shows currents during the 40-mV voltage step, showing the slowing of the current time course in response to consecutive MTSET applications. (E) The rate of MTSET modification at −100 mV (closed boxes) or 100 mV (open circles) was measured by fitting the current time course during the 40-mV voltage step (from data like in panel D) to a double exponential with τ1 = 70 ms (unmodified channels) and τ2 = 220 ms (modified channels). The amplitude of the slower component is plotted versus the cumulative MTSET exposure. The amplitude of the slower component is assumed to be proportional to the number of MTSET-modified 258C channels. The data were fitted with an exponential to yield the second order rate constant k for the MTSET reaction with R258C. k = 630/M/s for MTSET applied at −100 mV. No significant modification was seen when MTSET was applied only at 100 mV. n = 7. Error bars are SEM.

mutations, one gets a total of 24 e_0, about twice the 12–14 e_0 measured for WT Shaker K channels. This suggests that the effect of the neutralizations is not a simple removal of the charged residue. If, in addition, the charge neutralization also reduces the distance moved by the remaining charges in the transmembrane electrical field, then the contribution of the remaining charges to the gating charge will also be reduced. Indeed, in Shaker K channels it has been shown that some S4 charge neutralizations alter the extent of S4 movement (Baker et al., 1998). Also, in recent extended molecular dynamics (MD) simulations of Kv channels, it was shown that an S4 charge neutralization reduces the travel of S4 (Jensen et al., 2012). This could explain why the reduction of the total gating charge could be >1 e_0 per subunit (Aggarwal and MacKinnon, 1996; Seoh et al., 1996). We therefore tested whether some charge reduction in Hv channels also could be caused by an altered S4 movement, especially for the R255N mutation. Indeed, we show that the extent of motion is smaller in R255N channels compared with R255 channels. The curtailed movement of S4 in channels with the R255N mutation is most likely a contributing factor to the large reduction in effective gating charge for R255N because the smaller S4 movement leads to a smaller contribution of the two remaining S4 charges to the effective gating charge.

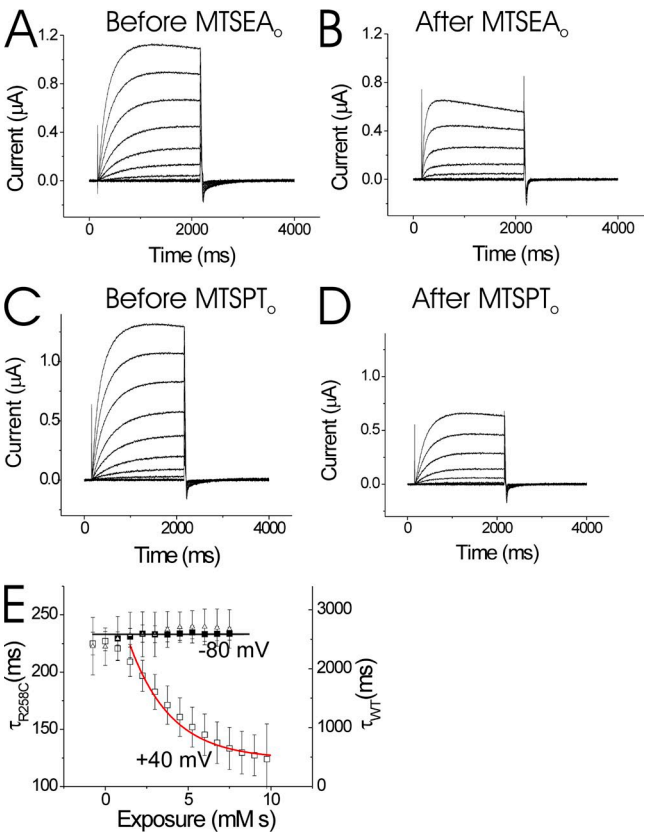

Figure 7. External MTS reagents modify R258C channels only in the open state. (A and B) Currents from an oocyte expressing 258C channels in response to voltage steps from −50 to 50 mV, before (A) and after (B) application of external MTSEA (150 μM). The holding potential was −60 mV. MTSEA was applied at 40 mV for 65 s in between the two recordings, showing that 258C is accessible to the external solution in open channels. pH_o = 7.4. (C and D) Currents from an oocyte expressing 258C channels in response to voltage steps from −50 to 50 mV, before (C) and after (D) external application of membrane-impermeable MTSPT. The holding potential was −60 mV. 1 mM MTSPT was applied at 40 mV for 65 s in between the two recordings, showing that 258C is accessible to the external solution in open channels. pH_o = 7.4. (E) Sequential 5-s applications of 150 μM MTSEA followed by 10-s washout was applied at the indicated voltage, and then the current was monitored in response to a 40-mV step every 30 s. The rate of MTSEA modification at −80 mV (closed boxes) or 40 mV (open boxes) was measured using the time constant for the current activation (left y axis) for the first 1,000 ms after the start of the 40-mV voltage step. The activation time constant versus the cumulative MTSEA exposure was plotted and fitted to an exponential. As a control, 150 μM MTSEA was applied at 40 mV on WT Ci-Hv1 channels, and the time constant for activation was monitored (open triangles; right y axis). No change in the activation time constant was noticed for WT Ci-Hv1 channels. Error bars are SEM.

In Fig. 5, we propose a model for S4 movement in Hv channels that is consistent with the accessibility data and the limiting slope measurements of the charge neutralizations. We base this model on the accessibility data and available crystal structures and molecular models of related Kv channels (Long et al., 2007; Pathak et al., 2007; Gonzalez et al., 2010). The contribution of each S4 charge can be estimated by assuming that the voltage is falling linearly over the inaccessible part of S4 (Fig. 5). This assumption results in an estimated total contribution of 2.6 e_0 for the three S4 charges (Fig. 5). A more realistic estimation of the contribution of each S4 charge for a similar model of Kv1.2 channels has been calculated using free energy perturbation (FEP)/MD simulations without the assumption of a linear voltage drop (Khalili-Araghi et al., 2010). In the Kv1.2 model, R2 contributes 0.7 e_0, R3 contributes 1.0 e_0, and R4 contributes 0.8 e_0 to the total gating charge in an isolated voltage-sensing domain. In our model of Hv channels, R1–R3 (R255, R258, and R261) correspond to R2–R4 in the Kv1.2 model. Assuming that Hv and the isolated voltage-sensing domain of Kv1.2 share similar structures, this model generates a gating charge per subunit of 2.5 e_0. Both the simple estimation based on a linear voltage drop and the more realistic FEP/MD simulation give a total gating charge (2.6 and 2.5 e_0, respectively) from the three S4 charges that is in reasonable agreement with the measured gating charge per subunit of 2.7 e_0 in Hv channels (Gonzalez et al., 2010), suggesting that no other charges contribute significantly to the gating charge in Hv channels. In conclusion, our data show for the first time that the three S4 charges are the main voltage-sensing residues responsible for the voltage dependence of Hv channels and that the extent of movement of these S4 charges is sufficient to explain the voltage dependence of opening in Hv channels.

We thank Drs. Ramon Latorre, Wolfgang Nonner, Karl Magleby, Fredrik Elinder, and Feng Qiu for comments on the manuscript.

This work was partially funded by a grant from the National Heart, Lung, and Blood Institute (R01-HL095920) to H.P. Larsson and Fondo Nacional de Desarrollo Científico y Tecnológico (FONDECYT) #1120802, ACT1104 to C. Gonzalez. Centro Interdisciplinario de Neurociencia de Valparaíso is a Millenium Institute.

Kenton J. Swartz served as editor.

Submitted: 9 July 2012
Accepted: 16 January 2013

REFERENCES

Aggarwal, S.K., and R. MacKinnon. 1996. Contribution of the S4 segment to gating charge in the Shaker K+ channel. *Neuron.* 16:1169–1177. http://dx.doi.org/10.1016/S0896-6273(00)80143-9

Almers, W. 1978. Gating currents and charge movements in excitable membranes. *Rev. Physiol. Biochem. Pharmacol.* 82:96–190. http://dx.doi.org/10.1007/BFb0030498

Baker, O.S., H.P. Larsson, L.M. Mannuzzu, and E.Y. Isacoff. 1998. Three transmembrane conformations and sequence-dependent displacement of the S4 domain in shaker K+ channel gating. *Neuron.* 20:1283–1294. http://dx.doi.org/10.1016/S0896-6273(00)80507-3

Bruening-Wright, A., F. Elinder, and H.P. Larsson. 2007. Kinetic relationship between the voltage sensor and the activation gate in spHCN channels. *J. Gen. Physiol.* 130:71–81. http://dx.doi.org/10.1085/jgp.200709769

Cherny, V.V., R. Murphy, V. Sokolov, R.A. Levis, and T.E. DeCoursey. 2003. Properties of single voltage-gated proton channels in human eosinophils estimated by noise analysis and by direct measurement. *J. Gen. Physiol.* 121:615–628. http://dx.doi.org/10.1085/jgp.200308813

Decoursey, T.E. 2003. Voltage-gated proton channels and other proton transfer pathways. *Physiol. Rev.* 83:475–579.

Gonzalez, C., H.P. Koch, B.M. Drum, and H.P. Larsson. 2010. Strong cooperativity between subunits in voltage-gated proton channels. *Nat. Struct. Mol. Biol.* 17:51–56. http://dx.doi.org/10.1038/nsmb.1739

Hirschberg, B., A. Rovner, M. Lieberman, and J. Patlak. 1995. Transfer of twelve charges is needed to open skeletal muscle Na+ channels. *J. Gen. Physiol.* 106:1053–1068. http://dx.doi.org/10.1085/jgp.106.6.1053

Iovannisci, D., B. Illek, and H. Fischer. 2010. Function of the HVCN1 proton channel in airway epithelia and a naturally occurring mutation, M91T. *J. Gen. Physiol.* 136:35–46. http://dx.doi.org/10.1085/jgp.200910379

Jensen, M.O., V. Jogini, D.W. Borhani, A.E. Leffler, R.O. Dror, and D.E. Shaw. 2012. Mechanism of voltage gating in potassium channels. *Science.* 336:229–233. http://dx.doi.org/10.1126/science.1216533

Jiang, Y., A. Lee, J. Chen, V. Ruta, M. Cadene, B.T. Chait, and R. MacKinnon. 2003. X-ray structure of a voltage-dependent K+ channel. *Nature.* 423:33–41. http://dx.doi.org/10.1038/nature01580

Khalili-Araghi, F., V. Jogini, V. Yarov-Yarovoy, E. Tajkhorshid, B. Roux, and K. Schulten. 2010. Calculation of the gating charge for the Kv1.2 voltage-activated potassium channel. *Biophys. J.* 98:2189–2198. http://dx.doi.org/10.1016/j.bpj.2010.02.056

Koch, H.P., T. Kurokawa, Y. Okochi, M. Sasaki, Y. Okamura, and H.P. Larsson. 2008. Multimeric nature of voltage-gated proton channels. *Proc. Natl. Acad. Sci. USA.* 105:9111–9116. http://dx.doi.org/10.1073/pnas.0801553105

Larsson, H.P., O.S. Baker, D.S. Dhillon, and E.Y. Isacoff. 1996. Transmembrane movement of the shaker K+ channel S4. *Neuron.* 16:387–397. http://dx.doi.org/10.1016/S0896-6273(00)80056-2

Lee, S.Y., J.A. Letts, and R. Mackinnon. 2008. Dimeric subunit stoichiometry of the human voltage-dependent proton channel Hv1. *Proc. Natl. Acad. Sci. USA.* 105:7692–7695. http://dx.doi.org/10.1073/pnas.0803277105

Lishko, P.V., I.L. Botchkina, A. Fedorenko, and Y. Kirichok. 2010. Acid extrusion from human spermatozoa is mediated by flagellar voltage-gated proton channel. *Cell.* 140:327–337. http://dx.doi.org/10.1016/j.cell.2009.12.053

Long, S.B., E.B. Campbell, and R. Mackinnon. 2005. Crystal structure of a mammalian voltage-dependent Shaker family K+ channel. *Science.* 309:897–903. http://dx.doi.org/10.1126/science.1116269

Long, S.B., X. Tao, E.B. Campbell, and R. MacKinnon. 2007. Atomic structure of a voltage-dependent K+ channel in a lipid membrane-like environment. *Nature.* 450:376–382. http://dx.doi.org/10.1038/nature06265

Mannuzzu, L.M., M.M. Moronne, and E.Y. Isacoff. 1996. Direct physical measure of conformational rearrangement underlying potassium channel gating. *Science.* 271:213–216. http://dx.doi.org/10.1126/science.271.5246.213

Okochi, Y., M. Sasaki, H. Iwasaki, and Y. Okamura. 2009. Voltage-gated proton channel is expressed on phagosomes. *Biochem. Biophys. Res. Commun.* 382:274–279. http://dx.doi.org/10.1016/j.bbrc.2009.03.036

Oxford, G.S. 1981. Some kinetic and steady-state properties of sodium channels after removal of inactivation. *J. Gen. Physiol.* 77:1–22. http://dx.doi.org/10.1085/jgp.77.1.1

Pathak, M.M., V. Yarov-Yarovoy, G. Agarwal, B. Roux, P. Barth, S. Kohout, F. Tombola, and E.Y. Isacoff. 2007. Closing in on the resting state of the Shaker K(+) channel. *Neuron.* 56:124–140. http://dx.doi.org/10.1016/j.neuron.2007.09.023

Ramsey, I.S., M.M. Moran, J.A. Chong, and D.E. Clapham. 2006. A voltage-gated proton-selective channel lacking the pore domain. *Nature.* 440:1213–1216. http://dx.doi.org/10.1038/nature04700

Ramsey, I.S., E. Ruchti, J.S. Kaczmarek, and D.E. Clapham. 2009. Hv1 proton channels are required for high-level NADPH oxidase-dependent superoxide production during the phagocyte respiratory burst. *Proc. Natl. Acad. Sci. USA.* 106:7642–7647. http://dx.doi.org/10.1073/pnas.0902761106

Sakata, S., T. Kurokawa, M.H. Nørholm, M. Takagi, Y. Okochi, G. von Heijne, and Y. Okamura. 2010. Functionality of the voltage-gated proton channel truncated in S4. *Proc. Natl. Acad. Sci. USA.* 107:2313–2318. http://dx.doi.org/10.1073/pnas.0911868107

Sasaki, M., M. Takagi, and Y. Okamura. 2006. A voltage sensor-domain protein is a voltage-gated proton channel. *Science.* 312:589–592. http://dx.doi.org/10.1126/science.1122352

Seoh, S.A., D. Sigg, D.M. Papazian, and F. Bezanilla. 1996. Voltage-sensing residues in the S2 and S4 segments of the Shaker K+ channel. *Neuron.* 16:1159–1167. http://dx.doi.org/10.1016/S0896-6273(00)80142-7

Sigg, D., and F. Bezanilla. 1997. Total charge movement per channel. The relation between gating charge displacement and the voltage sensitivity of activation. *J. Gen. Physiol.* 109:27–39. http://dx.doi.org/10.1085/jgp.109.1.27

Stimers, J.R., F. Bezanilla, and R.E. Taylor. 1985. Sodium channel activation in the squid giant axon. Steady state properties. *J. Gen. Physiol.* 85:65–82. http://dx.doi.org/10.1085/jgp.85.1.65

Tombola, F., M.M. Pathak, and E.Y. Isacoff. 2006. How does voltage open an ion channel? *Annu. Rev. Cell Dev. Biol.* 22:23–52. http://dx.doi.org/10.1146/annurev.cellbio.21.020404.145837

Tombola, F., M.H. Ulbrich, and E.Y. Isacoff. 2008. The voltage-gated proton channel Hv1 has two pores, each controlled by one voltage sensor. *Neuron.* 58:546–556. http://dx.doi.org/10.1016/j.neuron.2008.03.026

Tombola, F., M.H. Ulbrich, S.C. Kohout, and E.Y. Isacoff. 2010. The opening of the two pores of the Hv1 voltage-gated proton channel is tuned by cooperativity. *Nat. Struct. Mol. Biol.* 17:44–50. http://dx.doi.org/10.1038/nsmb.1738

Yang, N., A.L. George Jr., and R. Horn. 1996. Molecular basis of charge movement in voltage-gated sodium channels. *Neuron.* 16:113–122. http://dx.doi.org/10.1016/S0896-6273(00)80028-8

Zagotta, W.N., T. Hoshi, J. Dittman, and R.W. Aldrich. 1994. Shaker potassium channel gating. II: Transitions in the activation pathway. *J. Gen. Physiol.* 103:279–319. http://dx.doi.org/10.1085/jgp.103.2.279